Narrowing of the Flexural Phonon Spectral Line in Stressed Crystalline Two-Dimensional Materials

A. D. Kokovin,[1,2] V. Yu. Kachorovskii,[3] and I. S. Burmistrov[2,4]
[1]Moscow Institute of Physics and Technology, 141700 Moscow, Russia
[2]L. D. Landau Institute for Theoretical Physics, Semenova 1-a, 142432 Chernogolovka, Russia
[3]Ioffe Institute, 194021 Saint Petersburg, Russia
[4]Laboratory for Condensed Matter Physics, HSE University, 101000 Moscow, Russia

(Received 7 December 2023; revised 24 March 2024; accepted 15 July 2024; published 27 September 2024)

We develop the microscopic theory for the attenuation of out-of-plane phonons in stressed flexible two-dimensional crystalline materials. We demonstrate that the presence of nonzero tension strongly reduces the relative magnitude of the attenuation and, consequently, results in parametrical narrowing of the phonon spectral line due to stress-controlled suppression of the retardation effects in the dynamically screened inter phonon interaction. We predict the specific power-law dependence of the spectral-line width on temperature and tension. We speculate that suppression of the phonon attenuation by nonzero tension might be responsible for high quality factors of mechanical nanoresonators based on flexural two-dimensional materials.

DOI: 10.1103/PhysRevLett.133.136203

Following the discovery of graphene [1–3] and other atomically thin materials [4], flexible two-dimensional (2D) materials [5] have become at the focus of intense theoretical and experimental research. These 2D crystalline materials (2DCM) possess rich elastic physics due to an existence of out-of-plane deformations. Interplay of flexural strain and strong nonlinearities result in distinctive elastic properties—known as anomalous elasticity: nontrivial scaling of elastic modules with a system size controlled by universal exponent η, crumpling transition with increasing temperature, T and disorder, nonlinear Hooke's law, negative Poisson ratios, etc. [6–21].

These unusual phenomena predicted first for biological membranes are currently actively discussed in context of 2DCM [22–41]. As one of the most promising directions of research, 2DCM are explored as nanoelectromechanical systems (NEMS) with unexpectedly huge quality factors (10^2–10^4), increasing on decreasing T [42–47].

Huge quality factors of out-of-plane oscillations in 2DCM are very promising in view of fundamental analysis of interplay between optomechanics [48] and plasmonics [49]. By charging the electronic 2DCM with a static gate bias and applying an additional alternating electric field to the same or a different gate, it is possible to create tunable (by gate or stress) extra-high-quality plasmonic oscillators without damping by conventional momentum relaxation. This is a very appealing way to solve a long-standing fundamental problem for plasmonics.

Microscopically, an intrinsic momentum-dependent spectral line quality factor, Q_k, of flexural 2DCM is intimately related with the attenuation of flexural phonons due to their interaction mediated by in-plane phonons, while extrinsic sources are ineffective [50]. The key purpose of our Letter is to develop a microscopic theory of intrinsic flexural phonon attenuation due to nonlinear dynamically screened coupling between in-plane and out-of-plane phonons [51]. We will demonstrate that tension, σ, suppresses screening retardation effects, which are responsible for attenuation, thus drastically reducing the attenuation and hence resulting in a enhancement of the quality factor: $Q_k \propto \sigma^3$ for large σ.

This study is motivated both by above-mentioned experimental observation of huge quality factors in various 2DCM on perforated SiO_2 substrate: graphene [42–44], MoS_2 [45,52], WSe_2 [53], and $MoTe_2$ [52] (see Refs. [46,47] for a review), and by very recent direct experimental proof of the presence of attenuation in the phonon spectrum in graphene on a substrate [54]. In spite of clear request for the analytic theory of phonon attenuation in 2DCM, we are aware of a single theoretical work addressing the attenuation of flexural phonons in a free standing membrane with unphysical dimensionality $D = 4 - \epsilon$ with $\epsilon \ll 1$ used to control the theory [55].

We start with important comment on experimental situation. Contact between a membrane and a substrate imposes a stress on the membrane. Thus an existence of a nonzero tension σ acting on 2DCM is inevitable in a geometry of the experiment of Ref. [54] and in NEMS. We focus on an experimentally relevant range of T in which characteristics frequencies of flexural phonons are much smaller than T. We demonstrate that the presence of the tension strongly affects the flexural phonon attenuation and, consequently, the broadening of the phonon spectral line. The point is that σ enhances parametrically the real

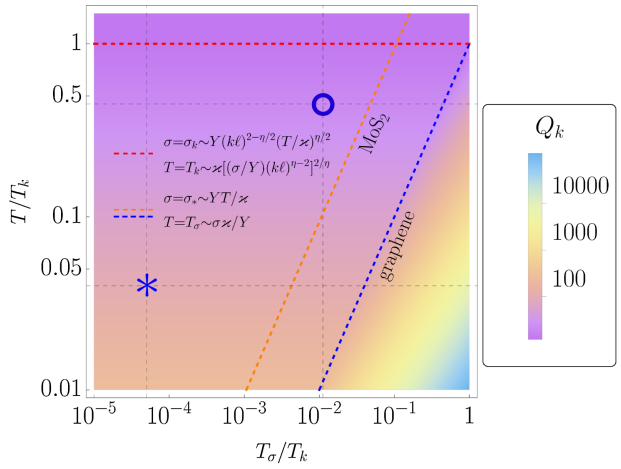

FIG. 1. The color density plot for dependence of the spectral line quality factor Q_k on temperature T and tension σ for wave vectors $k \ll 1/\ell = \sqrt{Y/\varkappa}$, where $\varkappa$ and Y are bending rigidity and Young's modulus, respectively. The "asterisk" and "circle" signs indicate the parameters corresponding to graphene and MoS_2 under realistic conditions (see discussions section), respectively.

part of the spectrum of flexural phonons also affecting the screened interaction between them. It is the latter that determines the phonon attenuation. The ratio of the real and imaginary parts of the spectrum of flexural phonons enhances parametrically in the presence of the nonzero σ. The predicted dependence of Q_k on T, σ, and wave vector, k, is shown in Fig. 1 and Table I. We discuss how our results might be related with high quality factors observed in out-of-plane dynamics of NEMS based on flexural 2DCM. We use units with $k_B = \hbar = 1$.

Model—The free energy describing thermal fluctuations in the flat phase of a 2D membrane can be written as $\mathcal{F} = \int d^2\boldsymbol{x}[\varkappa(\triangle\boldsymbol{r})^2/2 + \sigma(\nabla\boldsymbol{r})^2/2] + \mathcal{F}_{\rm el}$ [7,8]. Here $\varkappa$ is a bare bending rigidity while σ is an external tension. We use a $d = d_c + 2$ dimensional vector $\boldsymbol{r}$ to parametrize a point on the membrane in d-dimensional space. The 2D vector $\boldsymbol{x}$ parametrizes the point on the membrane with respect to some fixed plane. The elastic crystalline energy, $\mathcal{F}_{\rm el} = \int d^2\boldsymbol{x}[\mu{\rm tr}\hat{u}^2 + \lambda({\rm tr}\hat{u})^2/2]$, is expressed via the 2×2 strain tensor $\hat{u}$ with components $u_{\alpha\beta} = (\partial_\alpha\boldsymbol{r}\partial_\beta\boldsymbol{r} - \delta_{\alpha\beta})/2$. Here λ and μ are the Lamé parameters of 2DCM. $\mathcal{F}$ (with $d_c = 1$) describes 2DCM with D_{6h} (graphene) and D_{3h} (transition metal dichalcogenide monolayers) point groups. Following [9], we will use a standard expansion in $1/d_c$ to efficiently describe anharmonic effects. To study phonon dynamics we employ the imaginary time (τ) action $\mathcal{S} = \int_0^{1/T} d\tau[\int d^2\boldsymbol{x}\rho(\partial_\tau\boldsymbol{r})^2/2 + \mathcal{F}]$, where ρ denotes the membrane's mass density. To exploit the flatness of the membrane, we use the parametrization of the coordinates with in-plane ($\boldsymbol{u} = \{u_x, u_y\}$) and out-of-plane ($\boldsymbol{h} = \{h_1, \ldots, h_{d_c}\}$) displacements: $r_1 = \xi x + u_x$, $r_2 = \xi y + u_y$, and $r_{a+2} = h_a$ with $a = 1, \ldots, d_c$. Here $0 < \xi^2 < 1$ is the stretching factor which determines the ratio between projective and full area of the membrane. Following [6], we integrate out in-plane fluctuations $\boldsymbol{u}$ in harmonic approximation, and obtain the effective action for the flexural, out-of-plane phonons: $\mathcal{S}_{\rm eff} = \mathcal{S}_\xi + \mathcal{S}_0 + \mathcal{S}_{\rm int}$ [56]. Here $\mathcal{S}_0 = \sum_{\omega_n,k}[\rho\omega_n^2 + \sigma k^2 + \varkappa k^4]|\boldsymbol{h}_{\boldsymbol{k},\omega_n}|^2/2$ describes noninteracting flexural phonons. We use the following notation $\sum_{\omega_n,k} = T\sum_{\omega_n}\int d^2\boldsymbol{k}/(2\pi)^2$ for integration over momentum $\boldsymbol{k}$ and summation over bosonic Matsubara frequencies $\omega_n = 2\pi Tn$, $n \in \mathbb{Z}$. The quartic term [6]

$$\mathcal{S}_{\rm int} = \frac{Y}{8}\sum_{\Omega_m,\boldsymbol{q}\neq 0}\left|\sum_{\omega_n,\boldsymbol{k}} k_\perp^2 \boldsymbol{h}_{\boldsymbol{k}+\boldsymbol{q},\omega_n+\Omega_m}\boldsymbol{h}_{-\boldsymbol{k},-\omega_n}\right|^2, \qquad (1)$$

where $\boldsymbol{k}_\perp = [\boldsymbol{k}\times\boldsymbol{q}]/q$, describes the interaction of the flexural modes with transferred momentum $\boldsymbol{q}$ and frequency $\Omega_m = 2\pi Tm$, $m \in \mathbb{Z}$. $\mathcal{S}_{\rm int}$ emerges after integration over the in-plane phonons $\boldsymbol{u}$. The bare strength of interaction is determined by the Young's modulus $Y = 4\mu(\mu+\lambda)/(2\mu+\lambda)$.

Anomalous elasticity—The action $\mathcal{S}_0$ determines the bare spectrum of flexural phonons, $\omega_k = \sqrt{(\sigma k^2 + \varkappa k^4)/\rho}$. In the statics it is well established that the perturbation theory in powers of RPA-type screened interaction (see below) produces infrared logarithmic divergences that can be summed up by means of the renormalization group. Then, in the absence of the tension, $\sigma = 0$, a power law renormalization of the bending rigidity and Young's modulus emerges at low momenta [7,9],

$$\varkappa_k = \varkappa(kL_*)^{-\eta}, \qquad Y_k = Y(kL_*)^{-2+2\eta}, \qquad kL_* \ll 1. \qquad (2)$$

TABLE I. The results for the real (ω_k) and imaginary ($\gamma_k\omega_k$) parts of the flexural phonon spectrum in different regions of T and σ (see Fig. 1). We use $T_k \sim \varkappa[(\sigma/Y)(k\ell)^{\eta-2}]^{2/\eta}$, where $\ell = \sqrt{\varkappa/Y}$, and $T_\sigma \sim \sigma\varkappa/Y$. The corresponding scales for the tension are $\sigma_k \sim Y(k\ell)^{2-\eta}(T/\varkappa)^{\eta/2}$ and $\sigma_* \sim YT/\varkappa$.

	ω_k	$\gamma_k\omega_k$
$\sigma \ll \sigma_k$ $(T_k \ll T)$	$k^2\sqrt{\varkappa_k/\rho}$	$(\varkappa_k/\rho)^{\frac{1}{2}}k^2$
$\sigma_k \ll \sigma \ll \sigma_*$ $(T_\sigma \ll T \ll T_k)$	$k\sqrt{\sigma/\rho}$	$(\sigma/\rho)^{\frac{1}{2}}k^3\ell^2(Y/\sigma)^{1+\alpha}(T/\varkappa)^\alpha$
$\sigma_* \ll \sigma$ $(T \ll T_\sigma)$	$k\sqrt{\sigma/\rho}$	$(\sigma/\rho)^{\frac{1}{2}}k^3\ell^2(Y/\sigma)^3(T/\varkappa)^2$

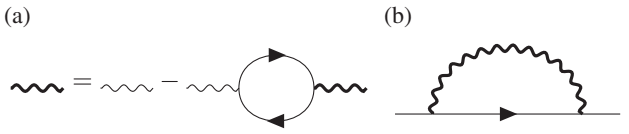

FIG. 2. (a) The RPA-type screened dynamical interaction. The wavy line denotes the bare interaction proportional to the Young's modulus. The solid line with arrow stands for the bare Green's function $G_{\boldsymbol{k}}(\omega)$. (b) The lowest order self-energy correction.

Here $L_* = \sqrt{32\pi\varkappa^2/(3d_c Y T)}$ is the so-called Ginzburg length. The magnitude of the universal exponent $\eta = 2/d_c + (73 - 68\zeta(3))/(27d_c^2) + \cdots$ is known for $d_c \gg 1$ from analytics [31]. In the case of $d_c = 1$ numerics yields $\eta \simeq 0.795 \pm 0.01$ [57]. The static renormalization affects dynamical properties making the true spectrum of flexural phonons less soft, $\omega_k \sim (\varkappa/\rho)^{1/2} k^2 (kL_*)^{-\eta/2}$ [7].

In a stressed membrane, $\sigma > 0$, there exists an additional length scale L_σ. For $\sigma < \sigma_* = \varkappa L_*^{-2}$ that scale is given as $L_\sigma = L_*(\sigma_*/\sigma)^{1/(2-\eta)}$ while $L_\sigma = L_*(\sigma_*/\sigma)^{1/2}$ for $\sigma \geq \sigma_*$. Provided $\sigma < \sigma_*$, the power-law renormalizations (2) hold for the interval $L_\sigma^{-1} \ll k \ll L_*^{-1}$ only. For region of small momenta, $kL_\sigma \ll 1$, the renormalization of the bending rigidity and Young's modulus become freezed to their magnitudes at $k = L_\sigma^{-1}$, [58]

$$\varkappa_\sigma = \varkappa(L_\sigma/L_*)^\eta, \qquad Y_\sigma = Y(L_\sigma/L_*)^{2-2\eta}. \tag{3}$$

However, these static renormalizations does not affect the spectrum of flexural phonons, $\omega_k \simeq \omega_k^{(\sigma)} = k\sqrt{\sigma/\rho}$, at low momenta, $kL_\sigma \ll 1$ [10,12,29]. It is this regime of low momenta we will below focus on.

Screened dynamical interaction—Similar to the static case the strong bare interaction between flexural phonons has to be screened. The retarded RPA-type screened interaction becomes $N_{\boldsymbol{q}}^R(\Omega) = (Y/2)/[1 + 3Y\Pi_{\boldsymbol{q}}^R(\Omega)/2]$ instead of $Y/2$ [see Fig. 2(a)]. We note that RPA is fully justified for $d_c \gg 1$. The retarded polarization operator can be expressed in a standard way in terms of two bare Green's functions. At $q \ll L_\sigma^{-1}$ we find the scaling form,

$$\Pi_{\boldsymbol{q}}^R(\Omega) = \frac{2Td_c}{3}\int \frac{d\omega d^2\boldsymbol{k}}{(2\pi)^3}\boldsymbol{k}_\perp^4 \left\{ G_{\boldsymbol{k}+\boldsymbol{q}}^R(\omega+\Omega)\frac{\mathrm{Im}G_{\boldsymbol{k}}^R(\omega)}{\omega} + G_{\boldsymbol{k}}^A(\omega)\frac{\mathrm{Im}G_{\boldsymbol{k}+\boldsymbol{q}}^R(\omega+\Omega)}{\omega+\Omega}\right\} \simeq \frac{T\mathcal{P}\left(\Omega/\omega_q^{(\sigma)}\right)}{32\pi\varkappa_\sigma^2 L_\sigma^{-2}}, \tag{4}$$

i.e., depending on the frequency Ω from the dimensionless combination $\Omega/\omega_q^{(\sigma)}$ only. Here we employed the classical limit of the boson equilibrium distribution function since we focus on the high temperature regime, $T \gg \omega_q, |\Omega|$. The bare Green's functions at $k \lesssim L_\sigma^{-1}$ are given as $G_{\boldsymbol{k}}^{R/A}(\omega) = 1/[\sigma k^2 + \varkappa_\sigma k^4 - \rho(\omega \pm i0)^2]$. For $\Omega \geq 0$, the function $\mathcal{P}(\Omega/\omega_q^{(\sigma)})$ is given by the integral representation

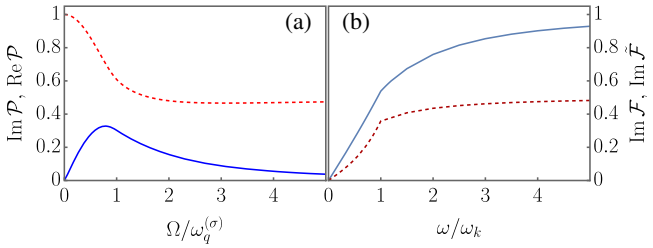

FIG. 3. (a) The real (red dashed curve) and imaginary (blue solid) parts of $\mathcal{P}(\Omega/\omega_q^{(\sigma)})$, see Eqs. (5) and (6). (b) The dependence of the imaginary part of the self-energy on frequency for $\omega \ll \omega_k/\sqrt{kL_\sigma}$. Solid blue and dashed red curves are for the function $\mathcal{F}$ and $\tilde{\mathcal{F}}$, see Eqs. (8) and (9), respectively.

(see Supplemental Material [60])

$$\mathcal{P}(\Omega/\omega_q^{(\sigma)}) = \int_0^1 dx\, \mathcal{X}\left(\Omega\sqrt{x}/\left(\omega_q^{(\sigma)}(2-x)\right)\right), \tag{5}$$

$$\mathcal{X}(z) = 1 - 2z^2 + \frac{4}{3}z^4 + \frac{4}{3}z|1-z^2|^{3/2}\begin{cases} i, & |z| \leq 1 \\ -1, & |z| > 1. \end{cases} \tag{6}$$

The real and imaginary part of the function $\mathcal{P}(z)$ are even and odd functions, respectively [see Fig. 3(a)]. We note that $\mathcal{P}(z) \simeq 1/2 - (2/(3z^2))[\ln z - i\pi/2]$ at $1 \ll z \ll 1/\sqrt{qL_\sigma}$. (For asymptotics at larger magnitudes of z see Ref. [60]).

In the limit of small momenta, $qL_\sigma \ll 1$, and of not too large frequencies, $|\Omega|/\omega_q \ll \sqrt{\sigma_*/\sigma}$, the screening dominates, $Y_\sigma \Pi_{\boldsymbol{q}}^R(\Omega) \gg 1$. Therefore, the screened interaction acquires the universal form determined by the inverse polarization operator $N_{\boldsymbol{q}}^R(\Omega) \simeq 1/[3\Pi_{\boldsymbol{q}}^R(\Omega)]$. Since $\Pi_{\boldsymbol{q}}^R(\Omega) \sim d_c$, the screened interaction becomes also weak, $\sim 1/d_c$, with respect to the number of out-of-plane modes.

Flexural phonon attenuation at $\sigma \ll \sigma_*$—The existence of $\mathrm{Im}\Pi_{\boldsymbol{q}}^R(\Omega) \neq 0$ results in the appearance of the imaginary part of the self energy for the exact Green's function of flexural phonons, $[\mathcal{G}_{\boldsymbol{k}}^R(\omega)]^{-1} = [G_{\boldsymbol{k}}^R(\omega)]^{-1} - \Sigma_{\boldsymbol{k}}^R(\omega)$. The latter is responsible for flexural phonon's attenuation. At $k \ll k_\sigma$, the lowest order self energy correction [see Fig. 2(b)] acquires the scaling form,

$$\Sigma_{\boldsymbol{k}}^R(\omega) = -4T\int \frac{d\Omega d^2\boldsymbol{q}}{(2\pi)^3}\boldsymbol{k}_\perp^4 \left[G_{\boldsymbol{k}+\boldsymbol{q}}^R(\omega+\Omega)\frac{\mathrm{Im}N_{\boldsymbol{q}}^R(\Omega)}{\Omega} + N_{\boldsymbol{q}}^A(\Omega)\frac{\mathrm{Im}G_{\boldsymbol{k}+\boldsymbol{q}}^R(\omega+\Omega)}{\omega+\Omega}\right] \simeq \frac{2\pi\varkappa_\sigma k^4}{d_c}\mathcal{F}\left(\frac{\omega}{\omega_k}\right). \tag{7}$$

Since $\Sigma^R \propto k^4$, its real part is completely negligible in comparison with the bare spectrum at $kL_\sigma \ll 1$. Albeit being small, $\mathrm{Im}\Sigma_{\boldsymbol{k}}^R(\omega)$ determines the attenuation of the flexural phonons. Next, we obtain ($z = \omega/\omega_k$, $\boldsymbol{r} = \boldsymbol{q}/k$)

$$\mathrm{Im}\mathcal{F}(z) = \frac{4z}{3\pi^2}\int \frac{d^2\boldsymbol{r}}{r^5}\frac{[\boldsymbol{n}\times\boldsymbol{r}]^4}{|\boldsymbol{n}+\boldsymbol{r}|^2}\sum_{s=\pm}\Phi\left(\frac{zs+|\boldsymbol{n}+\boldsymbol{r}|}{r}\right), \tag{8}$$

where $\Phi(x) = \mathrm{Im}\mathcal{P}(x)/[x|\mathcal{P}(x)|^2]$ and $\boldsymbol{n}$ is an auxiliary 2D unit vector. We note that Eq. (8) is applicable for $z \ll \sqrt{\sigma_*/\sigma}$ only since for larger magnitudes of z one cannot use the universal form of the screened interaction (see Ref. [60]). Using Eqs. (5) and (6), we find that $\mathrm{Im}\mathcal{F}(z) \simeq 0.5z$ for $z \ll 1$ and $\mathrm{Im}\mathcal{F}(z) \simeq 1$ at $z \gg 1$ (see Ref. [60]). The overall behavior of $\mathrm{Im}\mathcal{F}(\omega/\omega_k)$ is shown in Fig. 3(b). Since the real part of the self energy is proportional to k^4 it is completely negligible in comparison with σk^2.

Next, defining the attenuation coefficient as $\gamma_{\boldsymbol{k}} = \mathrm{Im}\Sigma^R_{\boldsymbol{k}}(\omega_{\boldsymbol{k}})/(\rho\omega^2_{\boldsymbol{k}})$, we find $\gamma_{\boldsymbol{k}} \simeq (3.2/d_c)(kL_\sigma)^2 \ll 1$. We note that this result holds at $\sigma \gg \sigma_k = \sigma_*(kL_*)^{2-\eta}$, otherwise L_σ becomes larger than $1/k$ for $\sigma \to 0$. In such a regime, the effect of tension becomes negligible and one finds $\gamma_k \sim 1$ [61]. Although above we presented the result for $\mathrm{Im}\Sigma^R_{\boldsymbol{k}}(\omega)$ in the lowest order in $1/d_c$, they are in fact completely general. The point is that the exact Green's function satisfies the Ward-Takahashi identity, $\lim_{\omega,k\to 0}[\mathcal{G}^R_{\boldsymbol{k}}(\omega)]^{-1} = \sigma k^2$ [10,12,29]. It forbids corrections to the self-energy of the type $k^2 f(\omega/\omega_k)$. Therefore, the functional form for the self-energy correction given by Eq. (7) is quite general and holds for all $d_c \geqslant 1$.

Flexural phonon attenuation at $\sigma \gg \sigma_*$—In that case, there is no power law renormalizations of $\varkappa$ and Y since $L_\sigma < L_*$. In addition, the screening of interaction is weak, so that $\mathrm{Im}N^R_{\boldsymbol{q}}(\Omega) \simeq -3(Y/2)^2\mathrm{Im}\Pi^R_{\boldsymbol{q}}(\Omega)$. We note that in this regime Eq. (7) reduces essentially to the Fermi golden rule expression for decay of the flexural phonon into three ones. Using Eq. (7), we find

$$\Sigma^R_{\boldsymbol{k}}(\omega) = \left(\frac{3}{32}\right)^2 \left(\frac{L_\sigma}{L_*}\right)^4 \frac{\varkappa k^4}{\pi d_c} \tilde{\mathcal{F}}\left(\frac{\omega}{\omega_k}\right), \tag{9}$$

where $\mathrm{Im}\tilde{\mathcal{F}}(z)$ is given by Eq. (8) but with $\Phi(x)$ substituted by $\tilde{\Phi}(x) = \mathrm{Im}\mathcal{P}(x)/x$. $\mathrm{Im}\tilde{\mathcal{F}}$ has linear asymptote at $z \ll 1$, $\mathrm{Im}\tilde{\mathcal{F}}(z) \simeq 0.2z$ and tends to the plateau, $\mathrm{Im}\tilde{\mathcal{F}}(z) \simeq 1/2$, at $1 \ll z \ll 1/\sqrt{qL_\sigma}$ [60]. The full dependence of $\mathrm{Im}\tilde{\mathcal{F}}$ on z is shown in Fig. 3(b). The above results imply that for $\sigma \gg \sigma_*$, the attenuation coefficient can be estimated as $\gamma_k \sim (Y/\sigma)^3(T/\varkappa)^2(k\ell)^2$, where $\ell = \sqrt{\varkappa/Y}$.

Spectral line quality factor—It is convenient to introduce the spectral line quality factor Q_k as inverse of the attenuation coefficient, $Q_k = 1/\gamma_k$. The Q_k factor characterizes the quality of the resonance in phonon spectral function at $\omega = \omega_k$. The results for the attenuation coefficient discussed above (see Table I) suggests the following behavior of Q_k for physical crystalline membrane (with $d_c = 1$),

$$Q_k \sim \begin{cases} 1, & \sigma \ll \sigma_k \text{ or } T_k \ll T, \\ \frac{(\sigma/Y)^{1+\alpha}(\varkappa/T)^\alpha}{(k\ell)^2}, & \sigma_k \ll \sigma \ll \sigma_* \\ & \text{or } T_\sigma \ll T \ll T_k, \\ (k\ell)^{-2}(\sigma/Y)^3(\varkappa/T)^2, & \sigma_* \ll \sigma \text{ or } T \ll T_\sigma, \end{cases} \tag{10}$$

where two temperature scales $T_k \sim \varkappa[(\sigma/Y)(k\ell)^{\eta-2}]^{2/\eta}$ and $T_\sigma = \varkappa\sigma/Y$ correspond to σ and σ_*, respectively. We emphasize that Eq. (10) predicts dramatic enhancement of the σ dependence of the quality factor when σ increases above σ_*. Sharp rise of the quality factor with tension, $Q_k \propto \sigma^3$, at $\sigma \gg \sigma_*$, is due to the stress-controlled suppression of the dynamically screened interaction. However, such increase of Q_k is partially compensated by a factor $1/\varkappa$. The unexpected appearance of $\varkappa$ for the regime $\sigma \gg \sigma_*$, where spectrum seems to be fully determined by σ, is connected with peculiar ultra-violet divergence of the dynamical polarization operator computed with linearly approximated spectrum $\omega^{(\sigma)}_q$ [60]. The temperature and tension dependencies of Q_k are controlled by the universal exponent $\alpha = \eta/(2-\eta) \simeq 0.67$. The overall behavior of the Q_k factor with respect to σ and T is sketched in Fig. 1. As naturally expected, the Q_k factor increases with decrease of temperature. Interestingly, a nonzero tension induces not only dependence on the tension but also significant temperature dependence of Q_k. Figure 1 demonstrates that Q_k increases with increase of σ. Thus the tension can serve as a tool to sharpen the phonon spectral line.

Discussions—Let us now estimate the spectral line quality factor Q_k. The characteristic tension σ_* for graphene is equal approximately 0.1 N/m. Taking build-in tension of a membrane to be $\sigma = 10^{-2}$ N/m (it corresponds to relative deformation $\sim 10^{-4}$), we find $L_\sigma \simeq 10$ nm. We choose the momentum $k \simeq 0.01$ nm^{-1} which corresponds approximately to 5×10^{-4} fraction of the distance between Γ and K points in graphene. We note that such a magnitude is on the lower boarder of current resolution of electron energy loss spectroscopy technique [62]. Then we obtain the estimate $Q_k \sim 10^2$ ("asterisk" sign in Fig. 1), that implies extremely narrow phonon spectral line. Similarly, one can estimate $Q_k \sim 10$ for MoS_2 ("circle" sign in Fig. 1) and other 2DCM listed in the introduction [60]. This implies that graphene is the best material for fabrication of NEMS.

It is tempting to apply our results for explanation of high quality factors of graphene-based NEMS [46,47]. For a stressed membrane of size L, one could naturally associate the resonance frequency of its oscillation as $\omega^{(\sigma)}_{k\sim 1/L}$. Then the spectral line quality factor $Q_{k\sim 1/L}$ determines the quality factor of the resonance. For $L_\sigma \ll L$, we obtain a large quality factor $Q_{k\sim 1/L} \sim (L/L_\sigma)^2 \gg 1$. In addition, that quality factor has temperature dependence, $Q_{k\sim 1/L} \sim T^{-\alpha}$. It resembles the $1/T$ dependence of the quality factor reported in the experiments [46,47]. The above estimate for graphene, $Q \sim 10^2$, is achieved for $L \sim 0.1$–1 μm, which is a typical size of NEMS.

As well known [63–71], the computation of broadening and decay for discrete levels is a tricky business. The phonon attenuation studied in our Letter can be thought to

be described like Fermi's golden rule for a decay of a flexural phonon with frequency ω_k into other three flexural phonons with the probability amplitude proportional to the screened interaction $N_{\boldsymbol{q}}^R(\Omega)$. The corresponding three-particle level spacing can be estimated as

$$\frac{1}{\Delta_3} = \prod_{j=1}^{3} \int \frac{L^2 d^2 \boldsymbol{k}_j}{(2\pi)^2} \delta(\omega_k - \omega_{k_1} - \omega_{k_2} - \omega_{k_3}) = \frac{\omega_k^5 L^6 \rho^3}{5!(2\pi\sigma)^3}. \tag{11}$$

In order for the decay to be efficient and Fermi's golden rule to be applicable, the three particle level spacing has to satisfy $\Delta_3 \ll \gamma_k \omega_k$ [65]. In the case, $L_*, L_\sigma \ll L$, the latter inequality transforms into the following condition $kL/\pi \gg (L/L_\sigma)^{1/4} \max\{1, (L_*/L_\sigma)^{1/2}\}$. Since $kL = 2\pi\sqrt{n^2+m^2}$ (where integers $n, m \geqslant 1$ in the case of zero boundary conditions for h), the quality factor of the resonance with $n, m \gg (L/L_\sigma)^{1/4} \max\{1, (L_*/L_\sigma)^{1/2}\}$ can be indeed estimated as $Q_{k\sim 1/L}$. In contrast, analysis of the low-frequency modes with $n \sim m \sim 1$ needs further development. For those modes we expect physics similar to that of Fermi-Pasta-Ulam-Tsingou problem [72]. We note, however, that discreteness can only enhance the quality factor $Q_{k\sim 1/L}$. Therefore, our present result can be considered as a lower bound for $Q_{k\sim 1/L}$ for low-frequency modes with $n \sim m \sim 1$.

Summary—To summarize, we developed the theory for the attenuation of out-of-plane phonons in stressed flexible 2D crystalline membranes. We found that the presence of nonzero tension strongly narrows the spectral line. We predicted the specific dependence of the flexural-phonon spectral-line width on temperature and tension. Such dependence can be used to benchmark our theory in experiments on phonon spectrum measurements by means of the high resolution electron energy loss spectroscopy. We proposed that suppression of phonon attenuation due to nonzero tension can be responsible for a huge magnitude of the quality factors of nanoresonators based on flexural 2D materials.

Existing experimental studies of the quality factor were focused on its T dependence. Comparing it with theory is complicated due to T variations in the membrane's in-built stress, caused by the details of setup fabrication. We propose an alternative way for experimentally verifying our theory: changing an external tension to exceed the in-built stress at the fixed T. This can be done using at least two techniques already used in experiments: making a 2DCM-based transistor and changing the gate voltage [42,73], or placing the membrane into a gas chamber with controlled pressure [74,75].

Finally, we list possible applications of the developed theory. Since an electromagnetic wave creates a tension in the illuminated membrane [76], our findings pave the way to controlling the phonon quality factor by placing a 2DCM into an optical cavity [77]. As discussed in the introduction, our work may give a boost to a field of acousto-plasmonics [78,79] in 2DCM. Such plasmonic-mechanical oscillators can be used as electrically and mechanically tunable radiation emitters and detectors thus opening a wide avenue for various optomechanical applications. A membrane under compressed stress can be in one of two mechanically bistable buckled states and hence creates a double-well potential for the coupled system of electrons and flexural phonons. Such bistable states show up in the single electron transport through a buckled membrane [80] and can be used for creation of stress-controlled quantum qubit [81]. The quantum coherence of such a qubit would directly depend on the quality factor of the flexural phonons.

Acknowledgments—The authors are grateful to Ya. Blanter and I. Gornyi for useful discussions. The work was funded in part by the Russian Ministry of Science and Higher Education (Project No. FFWR-2024-0015) and by the Basic Research Program of HSE. A. D. K. and I. S. B. acknowledge personal support from the Foundation for the Advancement of Theoretical Physics and Mathematics "BASIS". The work of V. Yu. K. was partially supported by the Russian Science Foundation (Grant No. 20-12-00147-П).

[1] K. S. Novoselov, A. K. Geim, S. V. Morozov, D. Jiang, Y. Zhang, S. V. Dubonos, I. V. Grigorieva, and A. A. Firsov, Electric field effect in atomically thin carbon films, Science **306**, 666 (2004).
[2] K. S. Novoselov, A. K. Geim, S. V. Morozov, D. Jiang, M. I. Katsnelson, I. V. Grigorieva, S. V. Dubonos, and A. A. Firsov, Two-dimensional gas of massless Dirac fermions in graphene, Nature (London) **438**, 197 (2005).
[3] Y. Zhang, Y.-W. Tan, H. L. Stormer, and P. Kim, Experimental observation of the quantum Hall effect and Berry's phase in graphene, Nature (London) **438**, 201 (2005).
[4] K. S. Novoselov and A. H. C. Neto, Two-dimensional crystals-based heterostructures: Materials with tailored properties, Phys. Scr. T **146**, 014006 (2012).
[5] *2D Materials: Properties and Devices*, edited by P. Avouris, T. F. Heinz, and T. Low (Cambridge University Press, Cambridge, England, 2017).
[6] D. Nelson and L. Peliti, Fluctuations in membranes with crystalline and hexatic order, J. Phys. (Paris) **48**, 1085 (1987).
[7] J. A. Aronovitz and T. C. Lubensky, Fluctuations of solid membranes, Phys. Rev. Lett. **60**, 2634 (1988).
[8] M. Paczuski, M. Kardar, and D. R. Nelson, Landau theory of the crumpling transition, Phys. Rev. Lett. **60**, 2638 (1988).
[9] F. David and E. Guitter, Crumpling transition in elastic membranes: Renormalization group treatment, Europhys. Lett. **5**, 709 (1988).

[10] J. Aronovitz, L. Golubovic, and T. C. Lubensky, Fluctuations and lower critical dimensions of crystalline membranes, J. Phys. (Paris) **50**, 609 (1989).

[11] E. Guitter, F. David, S. Leibler, and L. Peliti, Crumpling and buckling transitions in polymerized membranes, Phys. Rev. Lett. **61**, 2949 (1988).

[12] E. Guitter, F. David, S. Leibler, and L. Peliti, Thermodynamical behavior of polymerized membranes, J. Phys. (Paris) **50**, 1787 (1989).

[13] J. Toner, Elastic anisotropies and long-ranged interactions in solid membranes, Phys. Rev. Lett. **62**, 905 (1989).

[14] P. Le Doussal and L. Radzihovsky, Self-consistent theory of polymerized membranes, Phys. Rev. Lett. **69**, 1209 (1992).

[15] D. C. Morse, T. C. Lubensky, and G. S. Grest, Quenched disorder in tethered membranes, Phys. Rev. A **45**, R2151(R) (1992).

[16] D. R. Nelson and L. Radzihovsky, Polymerized membranes with quenched random internal disorder, Europhys. Lett. **16**, 79 (1991).

[17] L. Radzihovsky and D. R. Nelson, Statistical mechanics of randomly polymerized membranes, Phys. Rev. A **44**, 3525 (1991).

[18] D. C. Morse and T. C. Lubensky, Curvature disorder in tethered membranes: A new flat phase at $t = 0$, Phys. Rev. A **46**, 1751 (1992).

[19] D. Bensimon, D. Mukamel, and L. Peliti, Quenched curvature disorder in polymerized membranes, Europhys. Lett. **18**, 269 (1992).

[20] L. Radzihovsky and J. Toner, A new phase of tethered membranes: Tubules, Phys. Rev. Lett. **75**, 4752 (1995).

[21] L. Radzihovsky and J. Toner, Elasticity, shape fluctuations, and phase transitions in the new tubule phase of anisotropic tethered membranes, Phys. Rev. E **57**, 1832 (1998).

[22] E. I. Kats and V. V. Lebedev, Asymptotic freedom at zero temperature in free-standing crystalline membranes, Phys. Rev. B **89**, 125433 (2014).

[23] I. V. Gornyi, V. Y. Kachorovskii, and A. D. Mirlin, Rippling and crumpling in disordered free-standing graphene, Phys. Rev. B **92**, 155428 (2015).

[24] E. I. Kats and V. V. Lebedev, Erratum: Asymptotic freedom at zero temperature in free-standing crystalline membranes [Phys. Rev. B 89, 125433 (2014)], Phys. Rev. B **89**, 079904 (E) (2016).

[25] I. S. Burmistrov, I. V. Gornyi, V. Y. Kachorovskii, M. I. Katsnelson, and A. D. Mirlin, Quantum elasticity of graphene: Thermal expansion coefficient and specific heat, Phys. Rev. B **94**, 195430 (2016).

[26] I. V. Gornyi, V. Y. Kachorovskii, and A. D. Mirlin, Anomalous Hooke's law in disordered graphene, 2D Mater. **4**, 011003 (2016).

[27] A. Košmrlj and D. R. Nelson, Statistical mechanics of thin spherical shells, Phys. Rev. X **7**, 011002 (2017).

[28] P. Le Doussal and L. Radzihovsky, Anomalous elasticity, fluctuations and disorder in elastic membranes, Ann. Phys. (N.Y.) **392**, 340 (2018).

[29] I. S. Burmistrov, V. Y. Kachorovskii, I. V. Gornyi, and A. D. Mirlin, Differential Poisson's ratio of a crystalline two-dimensional membrane, Ann. Phys. (N.Y.) **396**, 119 (2018).

[30] I. S. Burmistrov, I. V. Gornyi, V. Y. Kachorovskii, M. I. Katsnelson, J. H. Los, and A. D. Mirlin, Stress-controlled Poisson ratio of a crystalline membrane: Application to graphene, Phys. Rev. B **97**, 125402 (2018).

[31] D. Saykin, I. Gornyi, V. Kachorovskii, and I. Burmistrov, Absolute Poisson's ratio and the bending rigidity exponent of a crystalline two-dimensional membrane, Ann. Phys. (N.Y.) **414**, 168108 (2020).

[32] D. R. Saykin, V. Y. Kachorovskii, and I. S. Burmistrov, Phase diagram of a flexible two-dimensional material, Phys. Rev. Res. **2**, 043099 (2020).

[33] O. Coquand, D. Mouhanna, and S. Teber, The flat phase of polymerized membranes at two-loop order, Phys. Rev. E **101**, 062104 (2020).

[34] A. Mauri and M. I. Katsnelson, Scaling behavior of crystalline membranes: An ϵ-expansion approach, Nucl. Phys. **B956**, 115040 (2020).

[35] A. Mauri and M. I. Katsnelson, Scale without conformal invariance in membrane theory, Nucl. Phys. **B969**, 115482 (2021).

[36] P. L. Doussal and L. Radzihovsky, Thermal buckling transition of crystalline membranes in a field, Phys. Rev. Lett. **127**, 015702 (2021).

[37] D. R. N. S. Shankar, Thermalized buckling of isotropically compressed thin sheets, Phys. Rev. E **104**, 054141 (2021).

[38] A. Mauri and M. I. Katsnelson, Perturbative renormalization and thermodynamics of quantum crystalline membranes, Phys. Rev. B **105**, 195434 (2022).

[39] S. Metayer, D. Mouhanna, and S. Teber, Three-loop order approach to flat polymerized membranes, Phys. Rev. E **105**, L012603 (2022).

[40] I. S. Burmistrov, V. Y. Kachorovskii, M. J. Klug, and J. Schmalian, Emergent continuous symmetry in anisotropic flexible two-dimensional materials, Phys. Rev. Lett. **128**, 096101 (2022).

[41] M. V. Parfenov, V. Y. Kachorovskii, and I. S. Burmistrov, Disorder-driven transition to tubular phase in anisotropic two-dimensional materials, Phys. Rev. B **106**, 235415 (2022).

[42] C. Chen, S. Rosenblatt, K. I. Bolotin, W. Kalb, P. Kim, I. K. H. L. Stormer, T. F. Heinz, and J. Hone, Performance of monolayer graphene nanomechanical resonators with electrical readout, Nat. Nanotechnol. **4**, 861 (2009).

[43] A. M. van der Zande, R. A. Barton, J. S. Alden, C. S. Ruiz-Vargas, W. S. Whitney, P. H. Q. Pham, J. Park, J. M. Parpia, H. G. Craighead, and P. L. McEuen, Large-scale arrays of single-layer graphene resonators, Nano Lett. **10**, 4869 (2010).

[44] T. Miao, S. Yeom, P. Wang, B. Standley, and M. Bockrath, Graphene nanoelectromechanical systems as stochastic-frequency oscillators, Nano Lett. **14**, 2982 (2014).

[45] R. van Leeuwen, A. Castellanos-Gomez, G. A. Steele, H. S. J. van der Zant, and W. J. Vestra, Time-domain response of atomically thin MoS_2 nanomechanical resonators, Appl. Phys. Lett. **105**, 041911 (2014).

[46] P. G. Steeneken, R. J. Dolleman, D. Davidovik, F. Alijani, and H. S. J. van der Zant, Dynamics of 2D material membranes, 2D Mater. **8**, 042001 (2021).

[47] P. F. Ferrari, S. Kim, and A. V. van der Zande, Nano-electromechanical systems from two-dimensional materials, Appl. Phys. Rev. **10**, 031302 (2023).

[48] M. Aspelmeyer, T. J. Kippenberg, and F. Marquardt, Cavity optomechanics, Rev. Mod. Phys. **86**, 1391 (2014).

[49] S. Maier, *Plasmonics—Fundamentals and Applications* (Springer, New York, 2007), 10.1007/0-387-37825-1.

[50] C. Seoánez, F. Guinea, and A. H. C. Neto, Dissipation in graphene and nanotube resonators, Phys. Rev. B **76**, 125427 (2007).

[51] D. Midtvedt, A. Croy, A. Isacsson, Z. Qi, and H. S. Park, Fermi-Pasta-Ulam physics with nanomechanical graphene resonators: Intrinsic relaxation and thermalization from flexural mode coupling, Phys. Rev. Lett. **112**, 145503 (2014).

[52] P. Zhang, Y. Jia, Z. Liu, and R. Yang, Strain-enhanced dynamic ranges in two-dimensional MoS_2 and $MoTe_2$ nanomechanical resonators, Appl. Phys. Rev. **11**, 011410 (2024).

[53] N. Morell, A. Reserbat-Plantey, I. Tsioutsios, K. G. Schädler, F. H. L. K. François Dubin, and A. Bachtold, High quality factor mechanical resonators based on WSe_2 monolayers, Nano Lett. **16**, 5102 (2016).

[54] J. Li, J. Li, J. Tang, Z. Tao, S. Xue, J. Liu, H. Peng, X.-Q. Chen, J. Guo, and X. Zhu, Direct observation of topological phonons in graphene, Phys. Rev. Lett. **131**, 116602 (2023).

[55] V. V. Lebedev and E. I. Kats, Long-scale dynamics of crystalline membranes, Phys. Rev. B **85**, 045416 (2012).

[56] Here the so-called zero-mode contribution $\mathcal{S}_\xi = \int d^2\boldsymbol{x} c_{\alpha\beta}\varepsilon_\alpha\varepsilon_\beta/(8T)$, where $c_{\alpha\beta} = \lambda + 2\mu\delta_{\alpha\beta}$ and $\varepsilon_\alpha = \xi^2 - 1 + \sum_{\omega,\boldsymbol{k}} k_\alpha^2 |h_{\boldsymbol{k},\omega}|^2$.

[57] A. Tröster, Fourier Monte Carlo simulation of crystalline membranes in the flat phase, J. Phys. Conf. Ser. **454**, 012032 (2013).

[58] In this work we neglect weak logarithmic depedence of $\varkappa$ on momentum for $kL_\sigma \ll 1$ [59].

[59] A. Košmrlj and D. R. Nelson, Response of thermalized ribbons to pulling and bending, Phys. Rev. B **93**, 125431 (2016).

[60] See Supplemental Material at http://link.aps.org/supplemental/10.1103/PhysRevLett.133.136203 for details of calculation of the polarization operator and the self-energy, and for estimates of quality factors of different flexible materials.

[61] A. D. Kokovin and I. S. Burmistrov, companion paper, Attenuation of flexural phonons in free-standing crystalline two-dimensional materials, Phys. Rev. B **110**, 125432 (2024).

[62] X. Zhu, Y. Cao, S. Zhang, X. Jia, Q. Guo, F. Yang, L. Zhu, J. Zhang, E. W. Plummer, and J. Guo, High resolution electron energy loss spectroscopy with two-dimensional energy and momentum mapping, Rev. Sci. Instrum. **86**, 083902 (2015).

[63] U. Sivan, Y. Imry, and A. G. Aronov, Quasi-particle lifetime in a quantum dot, Europhys. Lett. **28**, 115 (1994).

[64] Y. M. Blanter, Electron-electron scattering rate in disordered mesoscopic systems, Phys. Rev. B **54**, 12807 (1996).

[65] B. L. Altshuler, Y. Gefen, A. Kamenev, and L. S. Levitov, Quasiparticle lifetime in a finite system: A nonperturbative approach, Phys. Rev. Lett. **78**, 2803 (1997).

[66] A. D. Mirlin and Y. V. Fyodorov, Localization and fluctuations of local spectral density on treelike structures with large connectivity: Application to the quasiparticle line shape in quantum dots, Phys. Rev. B **56**, 13393 (1997).

[67] P. G. Silvestrov, Decay of a quasiparticle in a quantum dot: The role of energy resolution, Phys. Rev. Lett. **79**, 3994 (1997).

[68] P. G. Silvestrov, Stretched exponential decay of a quasiparticle in a quantum dot, Phys. Rev. B **64**, 113309 (2001).

[69] N. Auerbach and V. Zelevinsky, Super-radiant dynamics, doorways and resonances in nuclei and other open mesoscopic systems, Rep. Prog. Phys. **74**, 106301 (2011).

[70] I. V. Gornyi, A. D. Mirlin, and D. G. Polyakov, Many-body delocalization transition and relaxation in a quantum dot, Phys. Rev. B **93**, 125419 (2016).

[71] I. V. Gornyi, A. D. Mirlin, M. Müller, and D. G. Polyakov, Absence of many-body localization in a continuum, Ann. Phys. (Berlin) **529**, 1600365 (2017).

[72] E. Fermi, J. R. Pasta, and S. Ulam, Studies of nonlinear problems, Technical Report No. LA-1940, Los Alamos Scientific Laboratory, Los Alamos, 1955.

[73] R. J. T. Nicholl, H. J. Conley, N. V. Lavrik, I. Vlassiouk, Y. S. Puzyrev, V. P. Sreenivas, S. T. Pantelides, and K. I. Bolotin, The effect of intrinsic crumpling on the mechanics of free-standing graphene, Nat. Commun. **6**, 9789 (2015).

[74] S. P. Koenig, N. G. Boddeti, M. L. Dunn, and J. S. Bunch, Ultrastrong adhesion of graphene membranes, Nat. Nanotechnol. **6**, 543 (2011).

[75] R. J. T. Nicholl, N. V. Lavrik, I. Vlassiouk, B. R. Srijanto, and K. I. Bolotin, Hidden area and mechanical nonlinearities in freestanding graphene, Phys. Rev. Lett. **118**, 266101 (2017).

[76] I. D. Avdeev, A. N. Poddubny, and A. V. Poshakinskiy, Resonant optomechanical tension and crumpling of 2d crystals, ACS Photonics **7**, 2547 (2020).

[77] X. Song, M. Oksanen, J. Li, P. J. Hakonen, and M. A. Sillanpää, Graphene optomechanics realized at microwave frequencies, Phys. Rev. Lett. **113**, 027404 (2014).

[78] R. Marty, A. Mlayah, A. Arbouet, C. Girard, and S. Tripathy, Plasphonics: Local hybridization of plasmons and phonons, Opt. Express **21**, 4551 (2013).

[79] L. H. G. Tizei, V. Mkhitaryan, H. Lourenço-Martins, L. Scarabelli, K. Watanabe, T. Taniguchi, M. Tencé, J.-D. Blazit, X. Li, A. Gloter, A. Zobelli, F.-P. Schmidt, L. M. Liz-Marzán, F. J. G. de Abajo, O. Stéphan, and M. Kociak, Tailored nanoscale plasmon-enhanced vibrational electron spectroscopy, Nano Lett. **20**, 2973 (2020).

[80] S. S. Evseev, I. S. Burmistrov, K. S. Tikhonov, and V. Y. Kachorovskii, Effect of elastic disorder on single-electron transport through a buckled nanotube, Phys. Rev. Res. **4**, 013068 (2022).

[81] M. Ezawa, S. Yasunaga, A. Higo, T. Iizuka, and Y. Mita, Universal quantum computation based on nano-electromechanical systems, Phys. Rev. Res. **5**, 023130 (2023).